

Article

Cost Consensus Algorithm Applications for EV Charging Station Participating in AGC of Interconnected Power Grid

Jun Tang ¹, Xiang Ma ², Ren Gu ¹, Zhichao Yang ³, Shi Li ¹, Chen Yang ¹ and Bo Yang ^{4,*}¹ State Grid Suzhou Power Supply Company, Suzhou 215004, China; 18020180880@163.com (J.T.);

pulincao_kust@sina.com (R.G.); fanger1119@kmust.edu.cn (S.L.); waiting.198611@gmail.com (C.Y.)

² NARI Nanjing Control System Co., Ltd., Nanjing 21006, China; yangboffg@sina.com³ School of Electrical Engineering, Southeast University, Nanjing 210096, China; 230198240@seu.edu.cn⁴ Faculty of Electric Power Engineering, Kunming University of Science and Technology, Kunming 650500, China

* Correspondence: yangbo_ac@outlook.com; Tel.: +86-183-1459-6103

Received: 14 October 2019; Accepted: 12 November 2019; Published: 14 November 2019



Abstract: In order to more effectively reduce the regulation costs of power grids and to improve the automatic generation control (AGC) performance, an optimization mathematical model of generation command dispatch for AGC with an electric vehicle (EV) charging station is proposed in this paper, in which a cost consensus algorithm for AGC is adopted. Particularly, virtual consensus variables are applied to exchange information among different AGC units. At the same time, the actual consensus variables are utilized to determine the generation command, upon which the flexibility of the proposed algorithm can be significantly enhanced. Furthermore, the implement feasibility of such an algorithm is verified through a series simulation experiments on the Hainan power grid in southern China, where the results demonstrate that the proposed algorithm can effectively realize an autonomous frequency regulation of EVs participating in AGC.

Keywords: electric vehicle charging station; cost consensus algorithm; automatic generation control; autonomous frequency regulation

1. Introduction

Power system frequency stability is an important indicator of the power system quality and safety [1,2], upon which power system frequency regulation is mainly achieved by automatic generation control (AGC), which can guarantee satisfactory frequency quality and safe operation of the electric power system by maintaining the real-time balance between power generation and loads of the electric power system. Besides, with large-scale intermittent energy such as wind energy [3] being connected to the power grid, higher requirements for frequency regulation [4] and spinning reserve capacity are in urgent need to balance the unexpected power disturbance [5] to alleviate power quality problems [6] and ensure the power systems can operate under a safe and economical condition [7]. Hence, the intermittent energy can be operated at their maximum power point [8] most of the time by various control techniques [9]. In particular, when numerous electric vehicles (EVs) are connected to the power grid, that is, vehicle to grid (V2G), the utilization of EVs to provide auxiliary services such as frequency regulation for power system will be a popular research topic.

With the decrease of battery equipment costs, the advancement of charging and discharging technology, the gradual improvement of charging infrastructure, and the successive issuance of government supporting policies, the growth of EVs has become an inevitable trend that has aroused widespread attention [10]. Moreover, when numerous EVs are connected to the power grid, they are

not only regarded as loads that can absorb electricity from the power grid, but can also be utilized as discharge units to provide electricity to the power grid. Hence, EVs can be regarded as a controllable energy storage equipment to participate in economic dispatch [11] and peak-load shifting [12]. Particularly, recent studies show that it is a promising V2G commercial operation mode [13] to provide a frequency regulation service for a power system via centralized or decentralized control [14,15]. According to the literature [16], compared with the traditional generators, the participation of EVs in frequency regulation has the advantages of short frequency regulation delay, low frequency regulation cost, as well as fast and accurate responses to frequency regulation instructions. Besides, the literature [17] proposed the concept of EV agents, which can realize cluster dispatching to numerous EVs to meet the demand of power system frequency regulation capacity. Meanwhile, the feasibility of EVs participating in power system frequency regulation can also be verified. Hence, through controlling the charging and discharging behaviour of large-scale EVs, a series of auxiliary services, for example, power system frequency regulation, can be provided to effectively smoothen the load fluctuations of the power grid and to eliminate excess intermittent energy [18], while the generation efficiency of the renewable energy can be maximized [19].

Generally speaking, the application of exchanging battery mode in bus and taxi charging stations can be regarded as a reasonable business mode to cope with the large-scale development of EVs. This is because a bus or taxi can directly exchange a fully charged battery from the charging station without waiting. Particularly, charging stations are always equipped with a large number of batteries, which means they possess high frequency regulation capacity through making full use of retired batteries [20]. Consequently, the charging stations can be regarded as independent EV agents to participate in the frequency regulation service [21], which is crucial for power quality adjustment [22], while the power quality parameters can be estimated by the curve fitting algorithm [23]. When multiple charging stations participate in the secondary power system frequency regulation, there are typically two critical steps: (a) assigning the total power command ΔP_{EV} of EV centralized control center to each charging station and (b) assigning the power command of the charging station to each battery in the station.

Nowadays, the studies on the participation of EV in power system frequency regulation are still insufficient, which means the majority of studies mainly focus on the AGC power allocation of EVs in the EV charging station. Besides, the relevant factors including frequency regulation price, charging cost, and charging demand are taken into consideration in the literature [24], in which an allocation model is proposed to maximize the benefits of an EV charging station. Moreover, the authors of [25] regarded the fairness of EV's participation in power system frequency regulation as the ultimate purpose, instead of maximizing the benefits of the EV charging station, upon which various optimization algorithms are proposed to fairly allocate the charging and discharging power of EV. Moreover, in order to avoid over-charging and over-discharging of batteries, the authors of [26] allocated frequency regulation power commands according to the proportional allocation method based on state-of-charge (SOC).

However, none of the above studies involves the AGC power distribution among EV charging stations. At present, the most convenient and practical method is to allocate the total power instruction ΔP_{EV} equally to each EV charging station according to the proportion of adjustable capacity. Because each EV charging station belongs to different agents and the cost of power system frequency regulation is various, the average distribution method of adjustable capacity cannot minimize the cost of power system frequency regulation. In addition, the method usually allocates the total power command ΔP_{EV} to each EV charging station by centralized control, which requires collecting the information of each EV charging station in the real-time. When the scale of EV charging station participating in system frequency regulation increases, communication blockage and other problems will often occur.

In order to adapt to the trend of distributed/centralized development of centralized AGC in a smart grid [27] with high-penetration renewables [28], a decentralized and autonomous intelligent power generation control framework [29] combined with multi-agent collaborative consensus

algorithm [30] was proposed. Hence, the decentralized autonomous problem of AGC power allocation in interconnected power grid can be effectively solved, while EV is not involved as distributed generators to participate in the system frequency regulation. Particularly, a consensus algorithm can make the variables to reach a consensus through the cooperation between agents and adjacent agents in a multi-agent network, which has been widely used in formation control, unmanned aerial vehicle (UAV) control [31], cluster [32], robot swarm navigation [33], and stable flocking [34]. Hence, this paper applies the consensus algorithm to the AGC power allocation for each EV charging station. In order to avoid battery over-charging or over-discharging and to prolong the lifespan of the battery, a proportional allocation method based on SOC [21] is adopted to solve the AGC power redistribution. Finally, the model of the Hainan power grid in south China is utilized to evaluate the specific performance of the proposed method. Compared with the previous works, the main novelty of this paper can be summarized as follows:

- The traditional AGC power allocation is implemented among the thermal and hydro power plants in a centralized manner. In contrast, this paper provides a framework of AGC power allocation with EV, while the control command of each EV charging station can be calculated in a decentralized way.
- The cost consensus algorithm is designed for the distributed AGC power allocation among multiple EV charging stations, which can effectively reduce the total adjustment cost via a deep collaboration between local adjacent EV charging stations.

The rest of this paper is organized as follows. The framework and mathematical modelling of AGC power dynamic allocation with EV charging stations are introduced in Section 2. The AGC power allocation strategy of charging stations based on consensus algorithm is developed and analyzed in Section 3. Comprehensive case studies and simulation results are demonstrated in Section 4. Lastly, the conclusions are illustrated in Section 5.

2. Architecture and Mathematical Model of Automatic Generation Control Power Allocation with Electric Vehicle Charging Stations

2.1. Auxiliary Frequency Regulation Architecture of EV Charging Station

In general, various operations are undertaken in the power grid to balance the dynamic power disturbance, such as the load-damping and generator inertia, primary frequency control, and secondary frequency control. Particularly, the first two operations generally execute within a second, while AGC usually refers to the secondary frequency control with the time cycle from 1 to 16 seconds [35]. Besides, the load frequency control (LFC) consists of the primary frequency control and the secondary frequency control. The framework of AGC power dynamic allocation with EV charging stations is demonstrated in Figure 1, which mainly consists of a dispatching center, EV centralized control center, EV charging station, and EV batteries.

The main responsibilities of the dispatching center are to collect the frequency deviation and tie-line power deviation of power systems, calculate the total power generation command ΔP_{Σ} , and assign ΔP_{Σ} to AGC power supply units and EV centralized control centers via some certain algorithms.

The centralized EV control center acts as the interaction bridge, which ensures the two-way energy flow between EVs and the power grid [36]. Basically, it uploads the information of each EV charging station, for example, the price of unit-adjusted electricity and real-time adjustable capacity of each EV charging station, to the dispatching center. Besides, it assigns the total power instruction ΔP_{EV} issued by the dispatching center to each EV charging power station. However, consider that the EV charging stations under the electricity market belong to different agents, and the price of unit-adjusted electricity is different when participating in the power system frequency regulation. Hence, on the basis of power grid company benefits, some AGC power allocation strategies should be adopted among different EV charging stations to minimize the regulation costs of the power grid company.

An EV charging station can be regarded as an EV agent, which can implement cluster dispatching to large-scale EV batteries to meet the demand of power grid frequency regulation capacity. Under such circumstances, an EV will be preferable to participate in AGC ancillary service if its charging

demand can be completely satisfied after the ancillary service period [32]. Hence, each EV should upload its maximum charging power, initial battery state of charge (SOC), expected SOC, connecting time, expected exit time, charging efficiency, and energy capability to the control center of EV charging stations. On the other hand, the control center of the EV charging station allocates the power instructions issued by the centralized control center of EV to each EV battery based on the information of EV batteries such as the charged state and adjustable capacity.

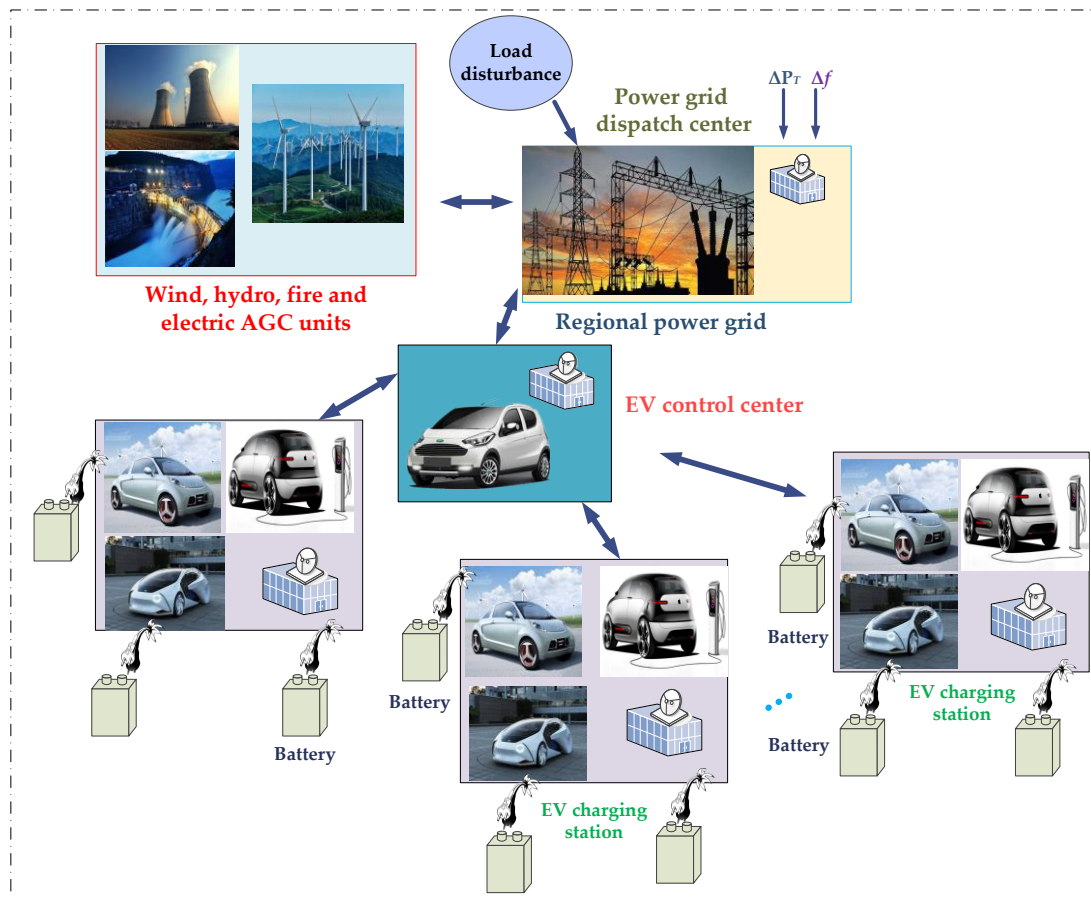


Figure 1. Framework of automatic generation control (AGC) power dynamic allocation with electric vehicle (EV) charging stations.

2.2. The Mathematical Model of AGC Power Dynamic Allocation with EV Charging Stations

Under the framework of auxiliary frequency regulation of EV charging stations, the regulation cost target is considered in AGC power allocation with EV charging stations. Particularly, it aims to distribute the total generation command of the EV centralized control center among all the EV charging stations. Moreover, the dynamic regulation features of all EVs are similar for AGC, as they can regulate their power outputs with a much faster response speed than the traditional thermal or hydro units. Hence, the objective function only regards the cost as the cost coefficient is the main difference between different EVs, which can be expressed as follows:

$$\min f = \sum_{i=1}^n \sum_{w=1}^{W_i} C_{iw} \Delta P_{iw}, \tag{1}$$

where f represents the total regulation cost target of the EV participating the frequency regulation; C_{iw} means the regulation cost coefficient of the w th battery of the i th EV charging station, which is the main parameter of each station; ΔP_{iw} is the power generation instruction assigned to the w th EV

battery of the i th EV charging station, which is also the decision variable; i represents the number of EV charging stations; W_i represents the total number of EV batteries of the i th EV charging station; and n is the number of charging stations.

To minimize the total regulation cost, the AGC power dynamic allocation should simultaneously satisfy various operation constraints, as follows:

(1) Power balance constraint: the total generation command should be balanced by all the charging stations, while the generation commands of each charging station should be equal to the sum of generation command of its controlled individual EVs, as follows:

$$\begin{cases} \Delta P_{EV\Sigma} = \sum_{i=1}^n \sum_{w=1}^{W_i} \Delta P_{iw} \\ \Delta P_i = \sum_{w=1}^{W_i} \Delta P_{iw}, i = 1, 2, \dots, n \end{cases}, \quad (2)$$

where $\Delta P_{EV\Sigma}$ denotes the general power generation instruction issued by the power grid dispatching center sent to the EV centralized control center; and ΔP_i represents the power generation instruction of the i th EV charging station, which is also the decision variable.

(2) Regulation direction constraint: the regulation direction of each charging station should be consistent with the total generation command, as follows:

$$-\Delta P_{EV\Sigma} \cdot \Delta P_{iw} < 0, i = 1, 2, \dots, n, m = 1, 2, \dots, W_i. \quad (3)$$

(3) Capacity constraint: both the regulation power and the SOC of each EV should be limited within their lower and upper bounds, and the direction of each charging station should be consistent with the total generation command, as follows:

$$\begin{cases} \Delta P_{iw}^{\min} \leq \Delta P_{iw} \leq \Delta P_{iw}^{\max} \\ SOC_{iw}^{\min} \leq SOC_{iw} \leq SOC_{iw}^{\max} \\ i = 1, 2, \dots, n, m = 1, 2, \dots, W_i \end{cases}, \quad (4)$$

where ΔP_{iw}^{\max} and ΔP_{iw}^{\min} denote the upper and lower limit, respectively, of the regulating capacity of the w th EV battery in the i th EV charging station, which are the known parameters; SOC_{iw}^{\max} and SOC_{iw}^{\min} are the upper and lower limit constraints, respectively, of the w th EV battery in the i th EV charging station allowed to participate the frequency regulation, which are the known parameters.

Under the framework of real-time dispatching of a power system that involves EV charging stations, the charging stations participate in power system frequency regulation with the expectation of obtaining certain benefits. Basically, according to the expected income and related costs of EV participation in power system frequency regulation, the open trading platform will be used to declare the price of unit adjustment electricity when the EV load participates in power system frequency regulation, which will be used to negotiate with the power grid dispatching center [37]. Under such circumstances, the power station acts as the seller of the frequency regulation service, while the dispatching center is regarded as the buyer. The buyer and seller are consentaneous to determine the transaction price and quantity via a one-to-one negotiation or one-to-many negotiation. After a successful negotiation, the buyer and seller need to sign the frequency regulation contract, in which the price of frequency regulation in the contract is the adjustment cost coefficient of the charging station, which is influenced by the frequency regulation capacity income, reverse discharge energy income, charging cost, and battery loss cost of charging stations. Moreover, the adjustment cost coefficient reduces with the increasing of frequency regulation capacity and reverse discharge energy income of charging stations, while the adjustment cost coefficient decreases with the decreasing of charging cost and battery loss cost of charging stations.

When a load disturbance occurs, in order to make the EV charging stations with lower regulation cost receive more active power insufficiency or surplus, the regulation cost is selected as the consensus state variable among EV charging stations. Besides, the power allocation algorithm with no leader and power deviation sharing mode is adopted. In order to avoid battery over-charging or over-discharging to reduce the influence on the lifespan of batteries, the SOC proportional allocation method is used to allocate the total power command of the EV charging station to each EV battery.

3. AGC Power Allocation Strategy of Charging Stations Based on Consensus Algorithm

3.1. Consensus Algorithm

A consensus algorithm is a decentralized control method that is mainly applied on multi-agents, which can cause the consensus state variables of the network to tend to be consentaneous through information interaction among intelligent agents. Particularly, considering that the communication among the agents needs a certain amount of time, the first order discrete consensus algorithm is adopted in this paper, while its iteration formula can be obtained as follows:

$$x_i[k + 1] = \sum_{j=1}^n d_{ij}x_j[k], \tag{5}$$

where x_i represents the information state of the i th agent; k denotes a discrete time series; and $d_{ij}[k]$ means the (i, j) element of row random matrix $D = [d_{ij}] \in R^{n \times n}$ at discrete time k , which can be defined by the following:

$$d_{ij}[k] = |l_{ij}| / \sum_{j=1}^n |l_{ij}|, \quad i = 1, 2, \dots, n, \tag{6}$$

where l_{ij} is the element of Laplace matrix L of multi-agent network topology G , which can be expressed as follows:

$$l_{ij} = \sum_{j=1, j \neq i}^n a_{ij}, \quad l_{ij} = -a_{ij}, \quad \forall i \neq j, \tag{7}$$

where a_{ij} represents the element of the adjacency matrix of G .

3.2. Charging Power Station AGC Power Allocation Based on Cost Consensus Algorithm

In order to make the charging station with lower adjustment cost bear with more power disturbance, the cost is selected as the consentaneous state variable. Hence, the adjustment cost r_i of the i th charging station can be written as follows:

$$r_i = C_i \cdot \Delta P_i, \tag{8}$$

where C_i represents the adjustment cost coefficient of the i th charging station.

For the purpose of ensuring the power balance and guaranteeing that all the EV charging stations can share the power deviation, the cost consensus variable r_i need to be updated as follows:

$$r_i[k + 1] \begin{cases} \sum_{j=1}^n d_{ij}[k]x_j[k] + \frac{\gamma \Delta P_{\text{error}}}{n}, & \Delta P_{\text{EV}\Sigma} > 0 \\ \sum_{j=1}^n d_{ij}[k]x_j[k] - \frac{\gamma \Delta P_{\text{error}}}{n}, & \Delta P_{\text{EV}\Sigma} < 0 \end{cases}, \tag{9}$$

where γ denotes the error adjustment factor, with $\gamma > 0$; and ΔP_{error} is the deviation between the total power instruction of EV centralized control center and the total power instruction of all EV charging stations, which can be defined by the following:

$$\Delta P_{\text{error}} = \Delta P_{\text{EV}\Sigma} - \sum_{i=1}^n \Delta P_i. \tag{10}$$

During the update of the consensus state variable, in order to gradually reduce the absolute value of power deviation, the adjustment cost consensus variable r_i should increase gradually if $\Delta P_{\text{EV}\Sigma}$ is positive. On the contrary, if $\Delta P_{\text{EV}\Sigma}$ is negative, the adjustment cost consensus variable r_i should decrease gradually.

After several iterations of Equation (9), the adjustment cost of each EV charging station tends to be consentaneous, while the convergence criteria can be given as follows:

$$\Delta P_{\text{error}} \leq \varepsilon. \tag{11}$$

During the optimization process, the power instruction assigned to an EV charging station may exceeds its reserve capacity limit. To guarantee that the generation command of each charging station can be limited within their lower and upper bounds, the following operation is designed into the optimization process:

$$\Delta P_i = \begin{cases} \Delta P_i^{\text{max}} = \sum_{i=1}^{M_i} \Delta P_{iw}^{\text{max}}, & \Delta P_i > \Delta P_i^{\text{max}} \\ \Delta P_i^{\text{min}} = \sum_{i=1}^{M_i} \Delta P_{iw}^{\text{min}}, & \Delta P_i < \Delta P_i^{\text{min}} \end{cases}, \tag{12}$$

where ΔP_i^{max} and ΔP_i^{min} represent the maximum and minimum standby capacity of the i th EV charging station, respectively.

Under such circumstances, the adjustment cost of the EV charging station also reaches the limits, as follows:

$$r_i = r_i^{\text{max}} = \begin{cases} C_i \cdot |\Delta P_i^{\text{max}}|, & \Delta P_i > \Delta P_i^{\text{max}} \\ C_i \cdot |\Delta P_i^{\text{min}}|, & \Delta P_i < \Delta P_i^{\text{min}} \end{cases}. \tag{13}$$

3.3. Virtual Consensus Variable and Actual Consensus Variable

When the power instruction of an EV charging station exceeds its reserve capacity limit, for the sake of avoiding updating the elements of a random matrix, the concepts of the virtual consensus variable and actual consensus variable are proposed in literature [38]. The virtual consensus variable is the information that the agent interacts with the neighboring agents in the multi-agent network, which is updated directly according to Equation (9) and Equation (10), without considering the capacity constraint of EV charging stations. Moreover, the actual consensus variable can reflect the real state of EV charging stations, which is obtained by Equation (12) and Equation (8), that is, the product of the actual assigned power instruction of the EV charging station and the corresponding adjustment cost coefficients, while the corresponding constraints are given by the following:

$$r_i^{\text{ac}} = \begin{cases} r_i^i, & \text{if } r_i^i < r_i^{\text{max}} \\ r_i^{\text{max}}, & \text{if } r_i^i \geq r_i^{\text{max}} \end{cases}. \tag{14}$$

3.4. Overall Design Flowchart

As shown in Figure 2, the AGC power allocation with EV mainly consists of two steps; that is, (a) the EV control center allocates the total power instruction $\Delta P_{\text{EV}\Sigma}$ to each charging station based on the cost consensus algorithm; and (b) it allocates the power instruction to each EV battery based on the SOC proportional allocation method.

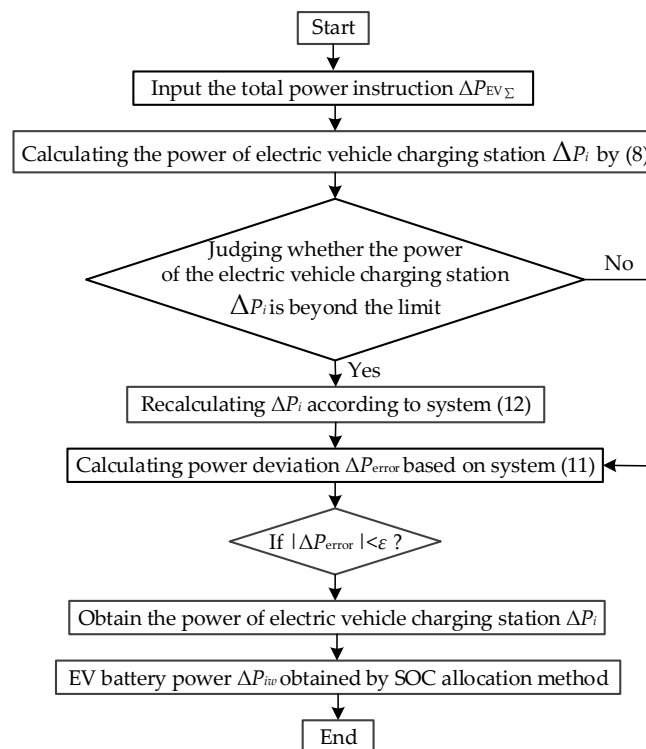


Figure 2. Flow chart of the proposed algorithm. SOC, state of charge.

4. Case Studies

4.1. System Model

According to the literature [39], from 2015 to 2020, China will give priority to the construction of more than 12,000 centralized charging stations for public transportation, sanitation, and logistics. Besides, more than 4.8 million decentralized charging piles will be established to meet the charging demand of public vehicles and private vehicles. In particular, EVs in the public services own the priority of changing electricity mode. On the basis of the load frequency control model of the Hainan power grid in southern China, the parameters of eight AGC units are tabulated in Table 1. According to the gross domestic product (GDP) ranking of each city and county in Hainan province in 2015, it is assumed that the top ten cities and counties (Haikou, Sanya, Chengmai, Danzhou, Qionghai, Wanning, Wenchang, Dongfang, Lingao, Lingshui) possess a large bus charging station, denoted by CS1~CS10, respectively. Each bus charging station can charge 120 bus batteries at the same time, and the models and parameters of all bus batteries are identical, with a battery capacity of 96 kWh. The communication topology of CS1~CS10 is demonstrated in Figure 3, and the adjustment cost coefficient is reasonably set according to the unit electricity price range $[\lambda_{bid,min}, \lambda_{bid,max}]$ corresponding to the lowest and highest expected income of EV agents, as given in Table 2. Besides, considering the influence of time-of-use electricity price, buses are charged twice a day. During the daytime, buses are charged for supplementary charging, while the charging period is 10:00–16:30 with a rated charging power of 135 kW. In addition, night charging is for unified centralized charging, while the charging period is 23:00–05:30 with a rated charging power of 21 kW. Therefore, it can be assumed that the total adjustable capacity of CS1~CS10 changes every 15 min [40] when participating in AGC power allocation, such that 96 periods are formed in a day, as illustrated in Figure 4. The maximum and minimum regulation capacity of CS1~CS10 under one period is shown in Table 2.

Table 1. Model parameters of automatic generation control (AGC) units in the Hainan power grid.

Unit	Class	Maximum Regulation Capacity (MW)	Minimum Regulation Capacity (MW)	Rate (MW·min ⁻¹)	Cost (yuan·(MWh) ⁻¹)
G1	Coal-fired unit	70	-70	3.5	132.83
G2	Coal-fired unit	210	-210	10.5	127.64
G3	Coal-fired unit	735	-735	36.75	181.42
G4	Liquefied Natural Gas unit	140	-140	14	226.78
G5	Liquefied Natural Gas unit	60	-60	6	233.91
G6	Hydropower unit	232	0	232	75.16
G7	Hydropower unit	52	0	52	73.67
G8	Hydropower unit	80	0	80	70.17

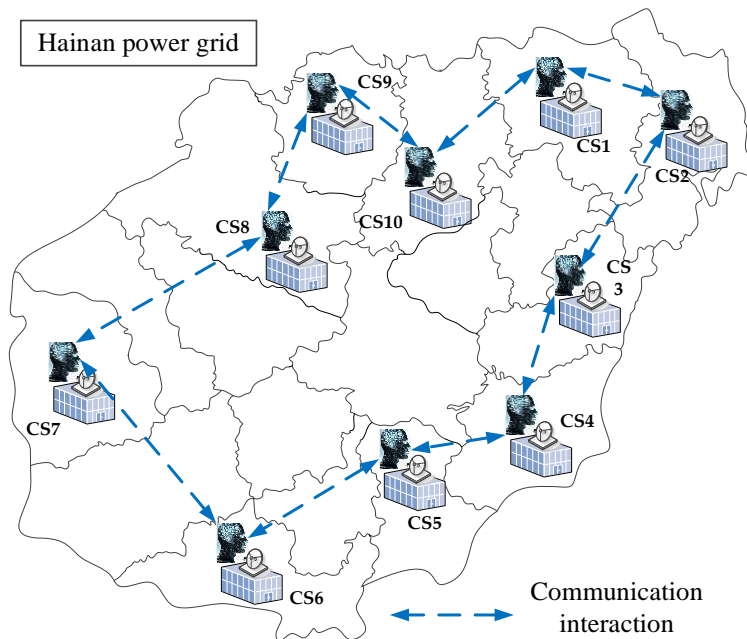


Figure 3. Communication network of charging stations (CSs) allocated in the Hainan power grid.

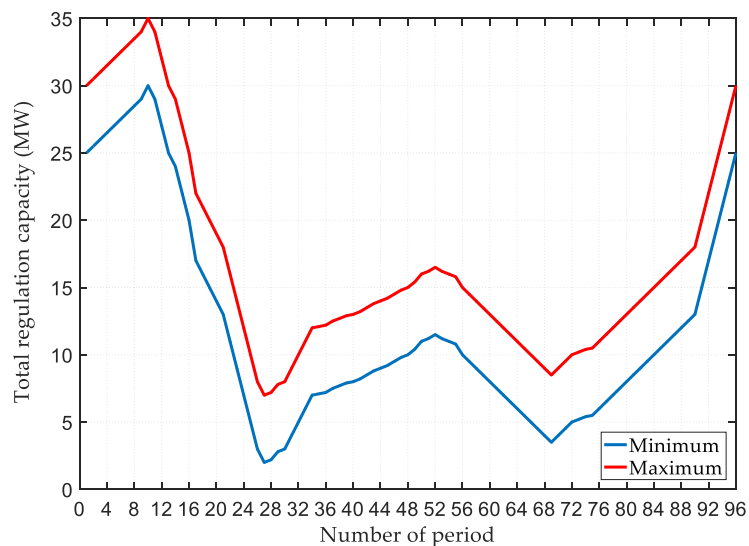


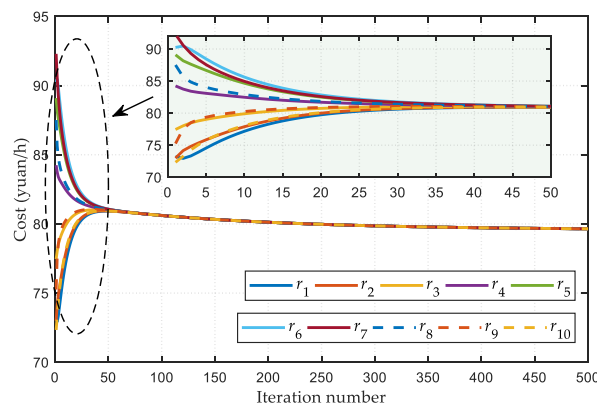
Figure 4. Total capacity power for regulation up and down of electric vehicle charging stations in one day.

Table 2. Regulation cost coefficient and total capacity power for regulation up and down in a period.

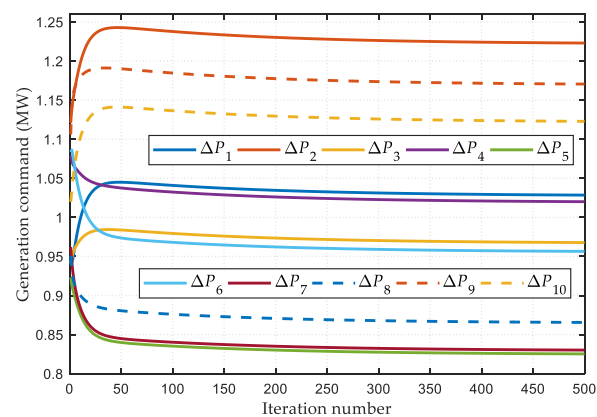
Charging Stations	The Adjustment Cost Coefficient C_i yuan (MW·h)	Maximum Regulation Capacity/MW	Minimum Regulation Capacity/MW
CS1	77.44	3	2.5
CS2	65.12	4.2	3.6
CS3	82.30	6.3	5.8
CS4	78.08	3.2	2.6
CS5	96.51	4.8	4.3
CS6	83.27	1.8	1.4
CS7	95.94	2.8	2.2
CS8	92.02	1.5	1.2
CS9	68.04	2.4	2.0
CS10	70.93	5	4.4

4.2. Discrete Consensus

On the basis of the above model and information topology, while taking the maximum and minimum adjustable capacity constraints of each charging station provided in Table 2 into consideration, the adjustment cost is considered as a consentaneous variable. Meanwhile, the convergence condition is $|\Delta P_{error}| \leq 0.01$ and the error adjustment factor γ is set to 0.5. When $\Delta P_{EV\Sigma} = 10$ MW, the convergence process of AGC power allocation for 10 charging stations based on the cost consensus algorithm is shown in Figure 5.



(a)

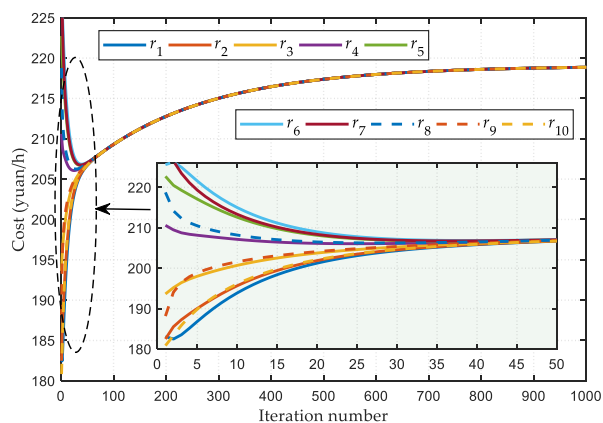


(b)

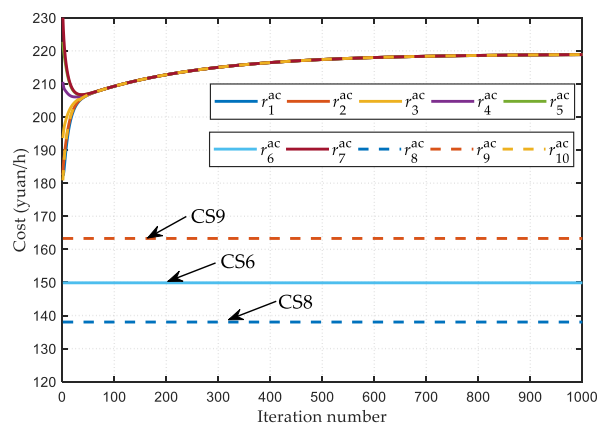
Figure 5. Consensus convergence process of regulation cost; (a) Convergence process of adjusting cost; (b) Convergence process of power generation in charging stations.

As demonstrated in Figure 5, one can readily observe that when the iteration number is 500, the regulation cost consensus variables of all charging power stations become identical, while the generation power of each charging power station converges at the same time, which is lower than 1.5 MW. Clearly, under the condition $\Delta P_{EV\Sigma} = 10$ MW, the generation power of all charging stations does not reach the upper limit of regulation capacity. Under such circumstances, the convergence process of the actual consensus variables is identical to that of the virtual consensus variables, as demonstrated in Figure 5a.

Figure 6 depicts the convergence process of adjusting the cost consensus algorithm when $\Delta P_{EV\Sigma} = 25$ MW, upon which one can readily observe that, with the increase of iteration numbers, the virtual regulation cost consensus variables of all rechargeable power stations tend to be consentaneous, while the generation power of each charging station also converges to a certain value. Owing to the restriction of maximum regulation capacity, the generation power of some charging stations has reached the limit, such as CS6, CS8, and CS9 shown in Figure 6c. Meanwhile, the actual consensus variables of these three charging stations also reach the limit, as shown in Figure 6b. Hence, this indicates that, because the concepts of the virtual consensus variable and actual consensus variable are introduced, even when the actual consensus variable reaches the limit value, the virtual consensus variable of all charging stations can still reach a consensus. More specifically, as the interactive information between different charging stations, the virtual consensus variable is not limited by the capacity constraint and is only used for cost consensus calculation by Equation (9). Through enough interactions, all the charging stations can reach a consensus on the virtual cost, while the power balance constraint can be satisfied. Therefore, the convergence of such an algorithm can be guaranteed by the interaction of virtual consensus variables among agents.

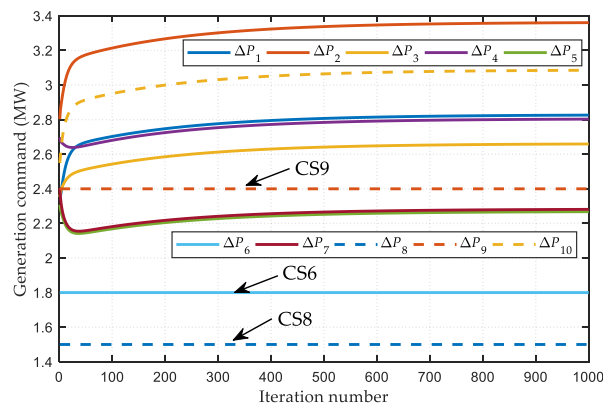


(a)



(b)

Figure 6. Cont.



(c)

Figure 6. Consensus convergence process of regulation cost; (a) Convergence process of virtual consensus variables; (b) Convergence process of actual consensus variables; (c) Convergence process of power generation in charging stations.

4.3. Random Disturbances

In order to further analyze the dynamic performance of the cost consensus algorithm for AGC power allocation with EV in practical applications, a random square wave load disturbance simulation is applied on the Hainan power grid while the wave period is 1000 s and the amplitude is no more than 150 MW (corresponding to 10% of the daily maximum load in Hainan province). Meanwhile, the simulation time is set to be 24 h. Besides, genetic algorithm (GA) [41,42], particle swarm optimization (PSO) [43,44], group search optimizer (GSO) [45], linear programming (LP) [46], and allocation algorithm based on the same adjustable capacity proportion are used for a fair and thorough performance comparison. In addition, the control period of AGC is nine seconds, while the total power command $\Delta P_{EV\Sigma}$ of EV centralized control center is obtained by offline static optimization based on GA, which aims to achieve a linear weighted minimization of the adjustment cost and a maximization of the climbing time of all AGC units in the whole control area. In order to further investigate the influence of the EV's participation in power system frequency regulation, coal-fired unit G3 and hydropower unit G6 are used to replace EV for further comparison, that is, the total power instruction $\Delta P_{EV\Sigma}$ of the EV centralized control center is all borne by coal-fired unit G3 or hydropower unit G6.

Table 3 demonstrates the control performance standard (CPS) index and adjustment cost when EVs participate in frequency regulation of the Hainan power grid under different algorithms, in which $|\Delta f|$, $|ACE|$ (automatic control error), CPS1, CPS2, and CPS are the average of the corresponding indicators within 24 h, while the cost is the total adjustment cost of all units in 24 h. From Table 3, one can readily find that the CPS index of the cost consensus algorithm is close to that of centralized algorithms such as GA, PSO, GSO, LP, and PROP, which further shows that the cost consensus algorithm is a feasible method for the decentralized control of AGC power allocation with EV in the power grid. In fact, the solved problem given in Equations (1)–(4) is linear, and its global optimum can be obtained by LP. In contrast, the proposed cost consensus algorithm is a distributed optimization method, for which it is difficult to obtain the global optimum, as it optimizes locally with the limited information. Although the heuristic algorithms (GA, PSO, and GSO) only search an approximate global optimum, they are still the good choice to be introduced for testing the performance of the proposed algorithm. In essence, the comparative algorithms, including GA, PSO, and GSO, are the meta-heuristic algorithm with various stochastic searching operations in nature. In order to reduce the optimization randomness and rapidly obtain a high-quality optimum, the local search weights of these algorithms are increased via setting their optimization parameters. Particularly, the crossover and mutation rates of GA are set to 0.9 and 0.05, respectively; the velocity weight of PSO is set to a dynamic value decreasing from 0.7

to 0.3; and the percentage of rangers is set to 10% for GSO. In addition, because the cost consensus algorithm uses the local information interaction of the agents to cause the consensus variables to tend to be consentaneous, it strongly depends on the optimization model. Hence, compared with centralized algorithms such as GA, PSO, GSO, and LP, its total adjustment cost is slightly higher.

Table 3. AGC performance indices obtained by different algorithms in the Hainan power grid in July. CPS, control performance standard; GA, genetic algorithm; PSO, particle swarm optimization; GSO, group search optimizer; LP, linear programming. The bold values are optimal values in this table.

Algorithm	$ \Delta f $ (Hz)	$ ACE $ (MW)	CPS1 (%)	CPS2 (%)	CPS (%)	Cost (10^3 yuan)
Cost consensus algorithm	9.0017×10^4	0.5176	199.9767	100	100	10.94
GA	9.0018×10^4	0.5177	199.9767	100	100	10.91
PSO	9.0014×10^4	0.5176	199.9767	100	100	10.92
GSO	9.0014×10^4	0.5176	199.9767	100	100	10.89
LP	9.2019×10^4	0.5723	199.9747	100	100	10.73
PROP	9.0014×10^4	0.5176	199.9767	100	100	10.95

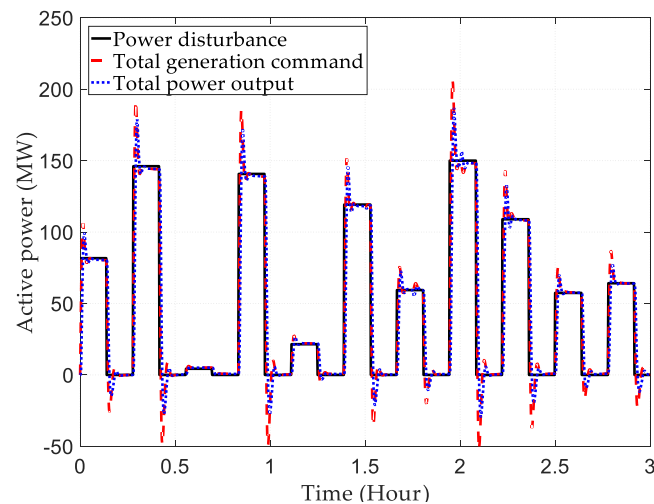
However, when the scale of the charging station increases, the centralized algorithms mentioned above have some distinct drawbacks, such as low calculation speed and weak optimum searching ability; thus, the 4–16 seconds’ time-scale requirement of AGC real-time control is hard to satisfy. However, the cost consensus algorithm still has the advantages of high convergence speed and stable optimization outcome, which represents higher practicability on engineering problems. Compared with other intelligence algorithms, the LP algorithm is a traditional optimization algorithm that can find the only definite optimal solution in the feasible domain, thus the total adjustment cost is the lowest. Besides, PROP adopts the fixed proportional allocation strategy based on the adjustable capacity, which lacks optimization objectives, such that its total adjustment cost is the highest among all the algorithms.

Table 4 shows the control performance standard index and total adjustment cost of the Hainan power grid without the participation of EV. The comparison between Tables 3 and 4 shows that, as the batteries of EV have a fast response speed, no climbing constraints, and low frequency regulation delay, the simulation results with EV participating in frequency regulation are better than those without EV. Hence, the participation of EV in AGC power allocation can effectively reduce the regional control deviation and restrain the load fluctuation. Meanwhile, as the time delay of the hydro-power unit is smaller than that of the thermal power unit and the climbing speed is higher, the simulation results are more desirable when the total power instruction $\Delta P_{EV\Sigma}$ of EV centralized control center is all borne by the hydro-power unit G6 rather than coal-fired unit G3. Besides, this also highlights that the participation of hydro-power in power system frequency regulation is beneficial to improve the CPS index and the economic performance index of the power grid.

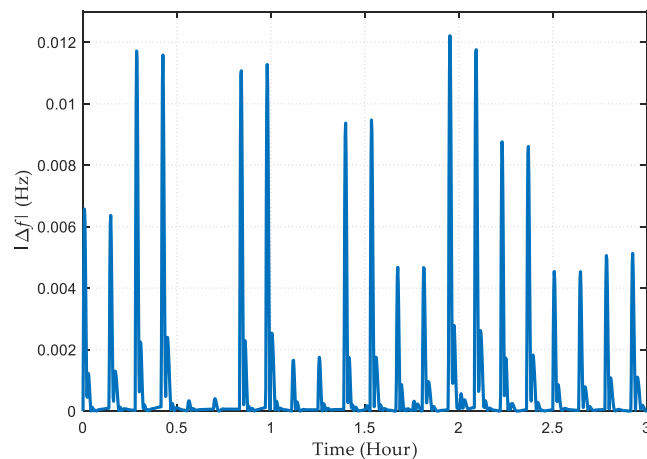
Table 4. AGC performance indices obtained by different scenarios without electric vehicles (EVs) in the Hainan power grid in July.

Scenarios	$ \Delta f $ (Hz)	$ ACE $ (MW)	CPS1 (%)	CPS2 (%)	CPS (%)	Cost (10^3 yuan)
Coal-fired unit G3 replaces EV	9.8239×10^4	0.5199	199.9753	100	100	11.73
Hydropower generator G6 replaces EV	9.3228×10^4	0.5209	199.9762	100	100	11.13

Figure 7 demonstrates the power tracking and frequency deviation curves (0–3 h) obtained by the cost consensus algorithm under random square wave load disturbance in the Hainan power grid. One can readily find that the total power instruction $\Delta P_{EV\Sigma}$ issued by the proportional–integral (PI) controller can effectively track the load disturbance, while the actual total output of the unit basically matches the load disturbance. Meanwhile, the frequency deviation of grid caused by the load disturbances can be maintained within a reasonable range, which can also quickly recover to the ideal value. The above results verify the feasibility of the cost consensus algorithm in the allocation of different charging stations.



(a)



(b)

Figure 7. Stochastic load disturbance in July; (a) active power regulation; (b) absolute value of frequency deviation.

5. Conclusions

This paper proposes a mathematical optimization model of AGC power allocation with EV charging stations. Besides, an AGC power allocation with EV based on the cost consensus algorithm is also developed, in which the main findings/contributions can be summarized as follows:

- 1) A feasible method for decentralized control is presented for AGC power allocation with EVs. After the virtual consensus variables and actual consensus variables are introduced, the cost consensus algorithm can be flexibly applied on the AGC power allocation of EV. Meanwhile, because such an algorithm possesses the superiorities of distributed calculation and simple updating rules, self-regulation of EV charging and discharging can be efficiently and effectively achieved.
- 2) The adjustment cost is regarded as the consentaneous state variable in the cost consensus algorithm, which means the charging stations with less adjustment cost receive more power disturbances. Particularly, such a strategy can effectively reduce the power grid frequency regulation cost and improve the control performance standard of a regional power grid.

Author Contributions: Preparation of the manuscript was performed by J.T., X.M., R.G., Z.Y., S.L., C.Y., and B.Y.

Funding: This research received no external funding.

Conflicts of Interest: The authors declare no conflict of interest.

Nomenclature

Variables

$\Delta P_{EV\Sigma}$	the general power generation instruction issued by the power grid dispatching center sent to the EV centralized control center, kW
C_{iw}	the adjustment cost coefficient of the w th battery of the i th EV charging station
ΔP_i	the power generation instruction of the i th EV charging station, kW
ΔP_{iw}	the power generation instruction assigned to the w th EV battery of the i th EV charging station, kW
ΔP_{iw}^{\max}	the upper limit of the regulating capacity of the w th EV battery in the i th EV charging station, kW
ΔP_{iw}^{\min}	the lower limit of the regulating capacity of the w th EV battery in the i th EV charging station, kW
SOC_{iw}^{\max}	the upper limit constraint of the w th EV battery in the i th EV charging station allowed to participate in the frequency regulation of the system, kW
SOC_{iw}^{\min}	the lower limit constraint of the w th EV battery in the i th EV charging station allowed to participate in the frequency regulation of the system, kW
i	the number of EV charging stations
W_i	the total number of EV batteries of the i th EV charging station
ΔP_{error}	the deviation between the total power instruction of EV centralized control center and the total power instruction of all EV charging stations, kW
ΔP_i^{\max}	the maximum standby capacity of the i th EV charging station, kW
ΔP_i^{\min}	the minimum standby capacity of the i th EV charging station, kW

System Parameters

f	the total adjustment cost target of the EV participating in the frequency regulation system, Hz
-----	---

Consensus algorithm parameters

x_i	the information state of the i th agent
k	discrete time series
r_i	the adjustment cost of the i th charging station
C_i	the adjustment cost coefficient of the i th charging station
γ	the error adjustment factor

Abbreviations

AGC	automatic generation control
V2G	vehicle to grid
EV	electric vehicle
GA	genetic algorithm
CPS	control performance standard
PSO	particle swarm optimization
GSO	group search optimizer
LP	linear programming

References

1. Arrillaga, J.; Watson, N.R.; Chen, S. *Power System Quality Assessment*; John Wiley & Sons: Hoboken, NJ, USA, 2000.
2. Fuchs, E.F. *Power Quality in Power Systems and Electric Machines University of Colorado*; ECEN 5787, Course Notes; Department of Electrical and Computer Engineering: Boulder, CO, USA, 2005.
3. Yang, B.; Yu, T.; Shu, H.; Dong, J.; Jiang, L. Robust sliding-mode control of wind energy conversion systems for optimal power extraction via nonlinear perturbation observers. *Appl. Energy* **2018**, *210*, 711–723. [[CrossRef](#)]
4. Arrillaga, J.; Smith, B.C.; Watson, N.R.; Wood, A.R. *Power System Harmonic Analysis*; John Wiley & Sons: Hoboken, NJ, USA, 1997.
5. Shen, Y.; Yao, W.; Wen, J.Y.; He, H.B.; Jiang, L. Resilient wide-area damping control using GrHDP to tolerate communication failures. *IEEE Trans. Smart Grid.* **2019**, *10*, 2547–2557. [[CrossRef](#)]

6. Caciotta, M.; Leccese, F.; Trifiro, A. From power quality to perceived power quality. In Proceedings of the IASTED International Conference on Energy and Power Systems, Chiang Mai, Thailand, 29–31 March 2006; pp. 94–102.
7. Liu, J.; Yao, W.; Wen, J.; Fang, J.; Jiang, L.; He, H.; Cheng, S.-J. Impact of Power Grid Strength and PLL Parameters on Stability of Grid-Connected DFIG Wind Farm. *IEEE Trans. Sustain. Energy* **2019**, *99*, 1. [[CrossRef](#)]
8. Yang, B.; Jiang, L.; Wang, L.; Yao, W.; Wu, Q. Nonlinear maximum power point tracking control and modal analysis of DFIG based wind turbine. *Int. J. Electr. Power Energy Syst.* **2016**, *74*, 429–436. [[CrossRef](#)]
9. Chen, J.; Yao, W.; Zhang, C.-K.; Ren, Y.; Jiang, L. Design of robust MPPT controller for grid-connected PMSG-Based wind turbine via perturbation observation based nonlinear adaptive control. *Renew. Energy* **2019**, *134*, 478–495. [[CrossRef](#)]
10. Wang, C.-S.; Stielau, O.H.; Covic, G.A. Design Considerations for a Contactless Electric Vehicle Battery Charger. *IEEE Trans. Ind. Electron.* **2005**, *52*, 1308–1314. [[CrossRef](#)]
11. Aziz, M.; Oda, T.; Mitani, T.; Watanabe, Y.; Kashiwagi, T. Utilization of Electric Vehicles and Their Used Batteries for Peak-Load Shifting. *Energies* **2015**, *8*, 3720–3738. [[CrossRef](#)]
12. Liu, H.; Ji, Y.; Zhuang, H.; Wu, H. Multi-Objective Dynamic Economic Dispatch of Microgrid Systems Including Vehicle-to-Grid. *Energies* **2015**, *8*, 4476–4495. [[CrossRef](#)]
13. Benedetto, A.; Sergio, B.; Luca, D.B.; Maria, D.; Giuseppe, F.; Michele, T. DC-microgrid operation planning for an electric vehicle supply infrastructure. *Appl. Sci.* **2019**, *9*, 2687.
14. Lingwen, G.; Ufuk, T.; Steven, H.L. Optimal decentralized protocol for electric vehicle charging. *IEEE Trans. Power Syst.* **2013**, *28*, 940–951.
15. Leccese, F. An overview on IEEE Std 2030. In Proceedings of the 11th International Conference on Environment and Electrical Engineering, Venice, Italy, 18–25 May 2012; pp. 340–345.
16. Dong, Q.L. Cluster control for EVs participating in grid frequency regulation by using virtual synchronous machine with optimized parameters. *Appl. Sci.* **2019**, *9*, 1924.
17. Han, S.; Han, S.; Sezaki, K. Development of an Optimal Vehicle-to-Grid Aggregator for Frequency Regulation. *IEEE Trans. Smart Grid* **2010**, *1*, 65–72.
18. Li, J.; Wang, S.; Ye, L.; Fang, J. A coordinated dispatch method with pumped-storage and battery-storage for compensating the variation of wind power. *Prot. Control. Mod. Power Syst.* **2018**, *3*, 2. [[CrossRef](#)]
19. Yang, B.; Zhong, L.; Zhang, X.; Shu, H.; Yu, T.; Li, H.; Jiang, L.; Sun, L. Novel bio-inspired memetic salp swarm algorithm and application to MPPT for PV systems considering partial shading condition. *J. Clean. Prod.* **2019**, *215*, 1203–1222. [[CrossRef](#)]
20. Xie, D.; Chu, H.; Lu, Y.; Gu, C.; Li, F.; Zhang, Y. The Concept of EV's Intelligent Integrated Station and Its Energy Flow. *Energies* **2015**, *8*, 4188–4215. [[CrossRef](#)]
21. Zhu, J.C.; Yang, Z.L.; Guo, Y.J.; Zhang, J.K.; Yang, H.K. Short-term load forecasting for electric vehicle charging stations based on deep learning approaches. *Appl. Sci.* **2019**, *9*, 1723. [[CrossRef](#)]
22. Leccese, F. Rome: A first example of perceived power quality of electrical energy. In Proceedings of the IASTED International Conference on Energy and Power Systems, Rome, Italy, 30 September–4 October 2007; pp. 169–176.
23. Caciotta, M.; Leccese, F.; Trifirò, A. Curve-fitting-algorithm (CFA) as power quality basic algorithm. In Proceedings of the 18th IMEKO World Congress 2006: Metrology for a Sustainable Development, Rio de Janeiro, Brazil, 17–22 September 2006; pp. 469–474.
24. Han, S.; Han, S.H.; Sezaki, K. Design of an optimal aggregator for vehicle-to-grid regulation service. In Proceedings of the 2010 Innovative Smart Grid Technologies (ISGT), Gothenburg, Sweden, 19–21 January 2010; pp. 1–8.
25. Escudero, G.J.; García, A.A.; Seco, G.G. Fair design of plug-in electric vehicles aggregator for V2G regulation. *IEEE Trans. Veh. Technol.* **2012**, *61*, 3406–3419. [[CrossRef](#)]
26. Li, J.; Gao, F.; Yan, G.; Zhang, T.; Li, J. Modeling and SOC estimation of lithium iron phosphate battery considering capacity loss. *Prot. Control. Mod. Power Syst.* **2018**, *3*, 5. [[CrossRef](#)]
27. Yang, B.; Yu, T.; Shu, H.; Zhang, Y.; Chen, J.; Sang, Y.; Jiang, L. Passivity-based sliding-mode control design for optimal power extraction of a PMSG based variable speed wind turbine. *Renew. Energy* **2018**, *119*, 577–589. [[CrossRef](#)]

28. Yang, B.; Zhang, X.; Yu, T.; Shu, H.; Fang, Z. Grouped grey wolf optimizer for maximum power point tracking of doubly-fed induction generator based wind turbine. *Energy Convers. Manag.* **2017**, *133*, 427–443. [[CrossRef](#)]
29. Liao, S.; Yao, W.; Han, X.; Wen, J.; Cheng, S. Chronological operation simulation framework for regional power system under high penetration of renewable energy using meteorological data. *Appl. Energy* **2017**, *203*, 816–828. [[CrossRef](#)]
30. Yang, H.; Li, S.; Li, Q.; Chen, W. Hierarchical distributed control for decentralized battery energy storage system based on consensus algorithm with pinning node. *Prot. Control. Mod. Power Syst.* **2018**, *3*, 6. [[CrossRef](#)]
31. Ruan, L.; Chen, J.; Guo, Q.; Jiang, H.; Zhang, Y.; Liu, D. A Coalition Formation Game Approach for Efficient Cooperative Multi-UAV Deployment. *Appl. Sci.* **2018**, *8*, 2427. [[CrossRef](#)]
32. Hanan, G.A.; Mohamed, S.K. Cumulative voting consensus method for partitions with variable number of clusters. *IEEE Trans. Pattern Anal. Mach. Intell.* **2008**, *30*, 160–173.
33. Gustavo, A.C.; Juan, M.C. Robot swarm navigation and victim detection using rendezvous consensus in search and rescue operations. *Appl. Sci.* **2019**, *9*, 1702.
34. Lee, D.; Spong, M.W. Stable Flocking of Multiple Inertial Agents on Balanced Graphs. *IEEE Trans. Autom. Control.* **2007**, *52*, 1469–1475. [[CrossRef](#)]
35. Zhang, X.S.; Yu, T.; Pan, Z.N.; Yang, B.; Bao, T. Lifelong learning for complementary generation control of interconnected power grids with high-penetration renewables and EVs. *IEEE Trans. Power Syst.* **2018**, *33*, 4097–4110. [[CrossRef](#)]
36. Cheng, Y.; Zhang, C. Configuration and operation combined optimization for EV battery swapping station considering PV consumption bundling. *Prot. Control. Mod. Power Syst.* **2017**, *2*, 276–293. [[CrossRef](#)]
37. Liu, H.; Huang, K.; Yang, Y.; Wei, H.; Ma, S. Real-time vehicle-to-grid control for frequency regulation with high frequency regulating signal. *Prot. Control. Mod. Power Syst.* **2018**, *3*, 13. [[CrossRef](#)]
38. Zhang, X.; Yu, T.; Yang, B.; Li, L. Virtual generation tribe based robust collaborative consensus algorithm for dynamic generation command dispatch optimization of smart grid. *Energy* **2016**, *101*, 34–51. [[CrossRef](#)]
39. National Development and Reform Commission of the PRC. *Electric Vehicle Charging Infrastructure Development Guide (2015–2020)*; National Development and Reform Commission of the PRC: Beijing, China, 9 October 2015.
40. Cai, H.; Chen, Q.; Guan, Z.; Huang, J. Day-ahead optimal charging/discharging scheduling for electric vehicles in microgrids. *Prot. Control. Mod. Power Syst.* **2018**, *3*, 9. [[CrossRef](#)]
41. Sze, S.L.; Bing, C.; Nik, R.N.I.; Hui, H.G.; Yeh, E.H. Switched-battery boost-multilevel inverter with GA optimized SHEPWM for standalone application. *IEEE Trans. Ind. Electron.* **2016**, *63*, 2133–2142.
42. Antonelli, A.; Giarnetti, S.; Leccese, F. Enhanced PLL system for Harmonic Analysis through Genetic Algorithm application. In Proceedings of the 11th International Conference on Environment and Electrical Engineering, Venice, Italy, 18–25 May 2012; pp. 328–333.
43. Umair, F.S.; Yoichi, S.; Sadiq, M.S. Multi-constrained route optimization for electric vehicles (EVs) using particle swarm optimization (PSO). In Proceedings of the 11th International Conference on Intelligent Systems Design and Applications, Córdoba, Spain, 22–24 November 2011; pp. 22–24.
44. Mangiatordi, F.; Pallotti, E.; Del Vecchio, P.; Leccese, F. Power consumption scheduling for residential buildings. In Proceedings of the 11th International Conference on Environment and Electrical Engineering, Venice, Italy, 18–25 May 2012; pp. 926–930.
45. Shayfull, Z.; Hazwan, M.H.M.; Nawati, M.A.M.; Ahmad, M.; Mohamad Syafiq, A.K.; Roslan, A.M. Warpage optimization on battery cover using glowworm swarm optimization (GSO). In Proceedings of the AIP Conference Proceedings, Noida, India, 17–19 January 2019.
46. Cardoso, G.; Stadler, M.; Siddiqui, A.; Marnay, C.; Deforest, N.; Barbosa-Povoa, A.; Ferrao, P. Microgrid reliability modeling and battery scheduling using stochastic linear programming. *Electr. Power Syst. Res.* **2013**, *103*, 61–69. [[CrossRef](#)]

